ELSEVIER

Physica A 269 (1999) 536–553

PHYSICA A

www.elsevier.com/locate/physa

# Rolling friction in the dynamic simulation of sandpile formation

Y.C. Zhou, B.D. Wright, R.Y. Yang, B.H. Xu, A.B. Yu *

*School of Materials Science and Engineering, The University of New South Wales, Sydney, NSW 2052, Australia*

Received 25 February 1999

**Abstract**

The contact between spheres results in a rolling resistance due to elastic hysteresis losses or viscous dissipation. This resistance is shown to be important in the three-dimensional dynamic simulation of the formation of a heap of spheres. The implementation of a rolling friction model can avoid arbitrary treatments or unnecessary assumptions, and its validity is confirmed by the good agreement between the simulated and experimental results under comparable conditions. Numerical results suggest that the angle of repose increases significantly with the rolling friction coefficient and decreases with particle size. 

*PACS:* 45.70.Cc; 45.50.-j; 45.70.Mg; 45.70.-n

*Keywords:* Static sandpiles; Granular compaction; Dynamics and kinematics of a particle and a system of particles; Granular flow; Mixing; Segregation and stratification; Granular systems

## 1. Introduction

The formation of a heap of particles is important in all industries dealing with particulate materials ranging from agricultural products such as flour and grains to minerals such as coal and metal ores. It is related to almost all typical phenomena associated with granular materials, and many aspects of heaping, including particle segregation [1], packing [2], and stress distribution [3,4], have been studied in the past. In recent years, many efforts have been made to understand the governing mechanisms involved, which are linked to important phenomena such as self-organisation [5,6] and stratification [7,8] that have stimulated the interest in particulate science and technology significantly [9–11].

* Corresponding author. Fax: +61-2-9385-5956.
*E-mail address:* a.yu@unsw.edu.au (A.B. Yu)

0378-4371/99/$ - see front matter 
PII: S0378-4371(99)00183-1

The bulk behaviour of a particle system depends on the collective interactions of individual particles. Therefore, it is very useful to study the heaping process on the particle scale. In the past, various computer simulation techniques have been developed for this purpose, including Monte Carlo [12–15], cellular automation [16], and granular dynamic simulations [17,18]. The latter is probably most realistic, because it explicitly takes into account not only the geometrical factors but also the forces involved. In recent years, it has been used by various investigators to study the formation of two-dimensional sandpiles [19–22]. However, to form a stable heap of particles with a finite angle of repose, special treatments or assumptions have to be employed in a simulation. For example, Lee and Herrmann [19] and Luding [20] ignored the rotation of particles or tangential forces, Elperin and Golshtein [21] set the velocities of all particles to zero after every 5000–15 000 iterations and Baxter et al. [22] started their simulation with a static substrate consisting of a row of equally spaced particles. Theoretically, such treatments are arbitrary and may distort reality, leading to inaccurate information.

The purpose of this paper is to propose a simulation method that can simulate the formation of a stable heap of spheres under three-dimensional conditions. The method is essentially that originally proposed by Cundall and Strack [17], but modified by introducing a rolling friction torque based on the experimental and theoretical analysis of Beer and Johnson [23] or Brilliantov and Poschel [24]. The effect of the rolling friction coefficient on the formation of a sandpile is studied in detail. The validity of the proposed modification is confirmed by the good agreement between the simulated and measured results under comparable conditions.

## 2. Simulation method

A particle can undergo translational and rotational motion, depending on the forces and torques acting on it, which may come from its interactions with neighbouring particles, with confining walls or substrates and with surrounding fluids. Strictly speaking, this movement is affected not only by the forces and torques originated from its neighbouring particles and vicinal fluid but also the particles and fluids far away through the propagation of disturbance waves. The complexity of such a process has defied any attempts to model this problem analytically. Even for the numerical approach, proper assumptions have to be made in order that this problem can be solved effectively without an excess requirement for computer memory or expensive iterative procedure. It has been established that if a time step is chosen to be less than a critical value, these forces and torques can be determined from the interactions between the particle and its immediate neighbours as well as vicinal fluid [17,25]. The interaction between particle and fluid and the long-range forces, such as van der Waals and electrostatic forces, can be ignored in the present work which deals with large particles in a static, low-viscosity fluid (air). Therefore, the governing equation for the translational motion

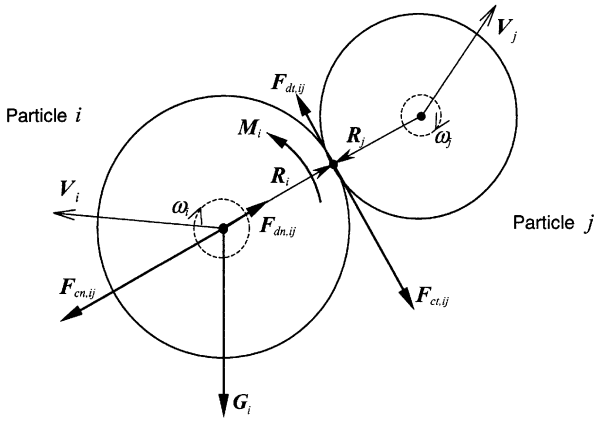


Fig. 1. Two-dimensional illustration of the forces acting on particle $i$ in contact with particle $j$.

of particle $i$ can be written as

$$m_i \frac{\mathrm{d}\boldsymbol{V}_i}{\mathrm{d}t} = m_i \boldsymbol{g} + \sum_{j=1}^{k_i} (\boldsymbol{F}_{c,ij} + \boldsymbol{F}_{d,ij}) , \tag{1}$$

where $m_i$ and $\boldsymbol{V}_i$ are the mass and velocity of particle $i$ and $t$ is time. As shown in Fig. 1, the forces involved are: the gravitational force, $m_i \boldsymbol{g}$, and the inter-particle forces between particles $i$ and $j$, which include the contact force, $\boldsymbol{F}_{c,ij}$, and the viscous contact damping force, $\boldsymbol{F}_{d,ij}$. These inter-particle forces are summed over the $k_i$ particles in contact with particle $i$.

The inter-particle forces act at the contact point between particles $i$ and $j$ rather than the particle centre and they will generate a torque, $\boldsymbol{T}_i$, causing particle $i$ to rotate. For a spherical particle of radius $R_i$, $\boldsymbol{T}_i$ is given by $\boldsymbol{T}_i = \boldsymbol{R}_i \times (\boldsymbol{F}_{ct,ij} + \boldsymbol{F}_{dt,ij})$, where $\boldsymbol{R}_i$ is a vector of magnitude $R_i$ from the mass centre of the particle to the contact point. Thus, the governing equation for the rotational motion of particle $i$ is

$$I_i \frac{\mathrm{d}\boldsymbol{\omega}_i}{\mathrm{d}t} = \sum_{j=1}^{k_i} \boldsymbol{T}_i , \tag{2}$$

where $\boldsymbol{\omega}_i$ is the angular velocity, and $I_i$ is the moment of inertia of particle $i$, given by $I_i = \frac{2}{5} m_i R_i^2$.

The inter-particle forces involved in Eq. (1) are determined from their normal and tangential components, i.e. $\boldsymbol{F}_{cn,ij}$ and $\boldsymbol{F}_{dn,ij}$, and $\boldsymbol{F}_{ct,ij}$ and $\boldsymbol{F}_{dt,ij}$, which depend on the normal and tangential deformations $\delta_n$ and $\delta_t$. A number of models can be used to quantify these forces. However, this is still an active research area, particularly for the tangential forces [26,27]. The present simulation is based on the most widely accepted force models [26–29], given in Table 1. These equations have been used by other investigators in two-dimensional studies of heaping [21,22]. However, as mentioned above, special treatments or assumptions were needed to form stable heaps in these early studies. While the formation of stable heaps is a complicated problem that is not

Table 1
Components of forces and torque acting on particle $i$

| Force | | Symbol | Equation |
|---|---|---|---|
| Normal forces | Contact | $\boldsymbol{F}_{cn,ij}$ | $-\frac{4}{3}E^*\sqrt{R^*}\delta_n^{3/2}\mathbf{n}$ |
| | Damping | $\boldsymbol{F}_{dn,ij}$ | $-c_n(\boldsymbol{V}_{ij}\bullet\mathbf{n})\mathbf{n}$ |
| Tangential forces | Contact | $\boldsymbol{F}_{ct,ij}$ | $-\frac{\mu_s\boldsymbol{F}_{cn,ij}}{\lvert\boldsymbol{\delta}_t\rvert}\left[1-\left(1-\frac{\min\{\lvert\boldsymbol{\delta}_t\rvert,\delta_{t,\max}\}}{\delta_{t,\max}}\right)^{\frac{3}{2}}\right]\boldsymbol{\delta}_t$ |
| | Damping | $\boldsymbol{F}_{dt,ij}$ | $c_t(\boldsymbol{V}_{ij}\times\mathbf{n})\times\mathbf{n}$ |
| Rolling | Torque | $\boldsymbol{T}_i$ | $\boldsymbol{R}_i\times(\boldsymbol{F}_{ct,ij}+\boldsymbol{F}_{dt,ij})$ |
| | Friction torque[a] | $\boldsymbol{M}_i$ | $-\mu_r\boldsymbol{F}_{cn,ij}\hat{\boldsymbol{\omega}}_i$ |
| Global | Gravity | $\boldsymbol{G}_i$ | $m_i\boldsymbol{g}$ |

where $\frac{1}{R^*}=\frac{1}{R_i}+\frac{1}{R_j}$, $E=\frac{E}{2(1-\nu^2)}$, $\boldsymbol{V}_{ij}=\boldsymbol{V}_j-\boldsymbol{V}_i+\boldsymbol{\omega}_j\times\boldsymbol{R}_j-\boldsymbol{\omega}_i\times\boldsymbol{R}_i$

$\hat{\boldsymbol{\omega}}_i=\frac{\boldsymbol{\omega}_i}{\omega_i}$, $\mathbf{n}=\frac{\boldsymbol{R}_i}{R_i}$, $\delta_{t,\max}=\mu_s\frac{2-\nu}{2(1-\nu)}\delta_n$

$\boldsymbol{\delta}_t$ is the vector of the accumulated tangential displacement between particles $i$ and $j$.

[a]Not considered in the previous work [17,21,22].

completely understood at present, an important factor that has been neglected in the earlier work is the rolling friction.

The relative rotation between contacting spheres or between a sphere and a wall in contact will produce a rolling resistance, because of the resulting elastic hysteresis loss or time-dependent deformation [30,31]. A few equations have been proposed for the calculation of this resistance [23,24,32–34]. For simplicity, the present work is based on two simple equations. The rolling resistance can be described in terms of a torque $\boldsymbol{M}_i$ that opposes to the rotation of the $i$th sphere. According to Beer and Johnson [23] this torque is given by

$$\boldsymbol{M}_i=-\mu_r F_{cn,ij}\hat{\boldsymbol{\omega}}_i \tag{3}$$

and according to Brilliantov and Poschel [24] the torque is given by

$$\boldsymbol{M}_i=-\mu_r' V_{\omega,ij}F_{cn,ij}\hat{\boldsymbol{\omega}}_i\,, \tag{4}$$

where $\mu_r$ or $\mu_r'$ is the rolling friction coefficient that is mainly related to material properties, and $V_{\omega,ij}$ is the magnitude of the relative tangential velocity contributed by the angular velocities at the contact point between particles $i$ and $j$, equal $|\boldsymbol{\omega}_j\times\boldsymbol{R}_j-\boldsymbol{\omega}_i\times\boldsymbol{R}_i|$.

Eqs. (3) and (4) actually represent two different treatments of rolling friction. In Eq. (3), the rolling friction is independent of the angular velocity and in Eq. (4), the rolling friction is directly proportional to the relative angular velocity. They will both be considered in this work, in order to understand their relative effectiveness. For convenience, in the following discussion, the implementation of Eq. (3) or (4) in the above dynamic model is referred to as Method A or B, respectively.

It is of interest to note that the rolling friction torque, expressed by Eq. (3), has been used by other investigators. In particular, Sakaguchi et al. [35] found that the rolling friction was important in simulating the arching phenomenon in discharging particles from a hopper; Iwashita and Oda [36] reported that the rolling friction significantly

affected shear band results. However, these studies are largely from the point of view of generating results comparable to the experimental observations; and the significance of rolling friction in the simulation of sandpile formation has not been recognised in the literature.

## 3. Results and discussion

### 3.1. Motion of a sphere on a flat plate

It is known that a sphere moving on a horizontal plate with an initial translational velocity will gradually loss its kinetic energy and finally stop after travelling a certain distance because of the resistance from its interaction with the plate. This simple fact has been used here as the first case to test the proposed approach. In particular, it is assumed that initially the sphere just touches the plate with an initial translational velocity of 1 m/s but no angular velocity; and the physical properties used are listed in Table 2. The time step used for the simulation is less than $2 \times 10^{-5}$ s, varying with sphere diameter [37].

Fig. 2 shows the increase of the distance traveled by a sphere with time. It can be seen that if the rolling friction coefficient is equal to zero, the distance increases linearly with time. This unphysical result stems from the fact that no resistance is available to stop the rolling of a sphere originally generated due to the contact force. As discussed above, this behaviour cannot be simply attributed to the inaccuracy in numerical treatments but in theoretical formulation. In fact, once a rolling friction torque, given by either Eq. (3) or (4), is introduced, the sphere will indeed stop after travelling a finite distance. Obviously, the maximum distance travelled should vary with the diameter of the sphere and the rolling friction coefficient. Fig. 3 shows the results, indicating that the distance increases linearly with particle size and decreases with the rolling friction coefficient. One interesting feature here is that if the rolling friction coefficient $\mu_r$ or $\mu_r'$ is higher than a critical value, about $10^{-3}$ m or s/rad, the

Table 2
Physical parameters used in the present simulations[a]

| Variable | Value |
|---|---|
| Particle density $\rho$ | 2500 kg/m$^3$ |
| Young's modulus of particle or wall $E$ | $10^6$ N/m$^2$ |
| Poisson ratio of particle or wall $v$ | 0.3 |
| Particle–particle friction coefficient $\mu_{s,\,pp}$ | 0.4 |
| Particle–wall friction coefficient $\mu_{s,\,pw}$ | 0.7 |
| Particle–particle damping coefficient $c_{pp}$ | 0.4 kg/s |
| Particle–wall damping coefficient $c_{pw}$ | 0.7 kg/s |

[a]In this work, it is assumed that $\mu_s = \mu_{s,\,pp}$ and $c_t = c_n = c_{pp}$ for contacts between particles, and $\mu_s = \mu_{s,\,pw}$ and $c_t = c_n = c_{pw}$ for contacts between particle and wall or plate.

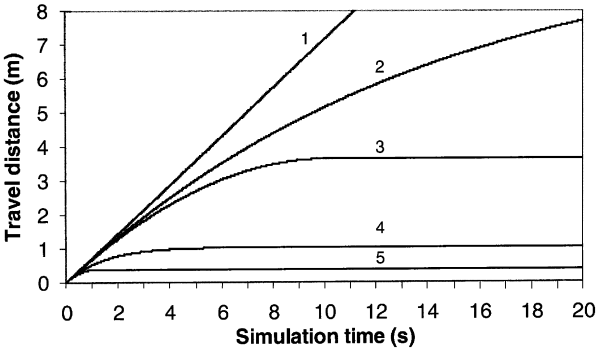


Fig. 2. Travel distance vs. time for a 10 mm sphere moving on a horizontal plate with an initial velocity (1 m/s) and different rolling friction coefficients: line 1, without rolling friction; line 2, $\mu_r' = 5 \times 10^{-4}$ s/rad (Method B); line 3, $\mu_r = 5 \times 10^{-4}$ m (Method A); line 4, $\mu_r' = 5 \times 10^{-3}$ s/rad (Method B); line 5, $\mu_r = 5 \times 10^{-3}$ m (Method A).

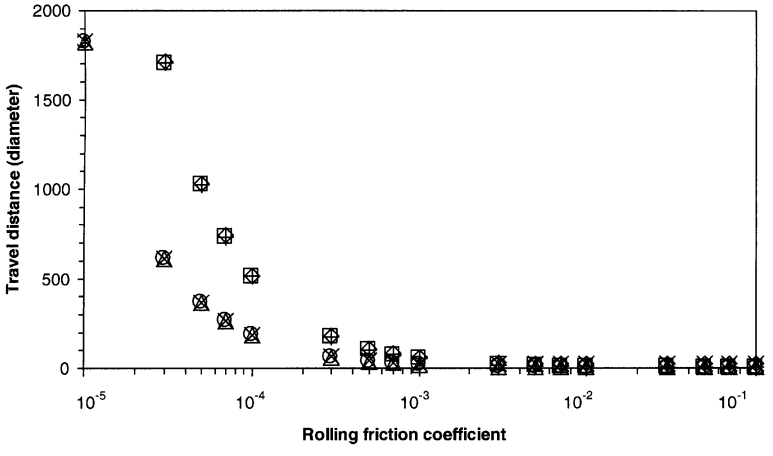


Fig. 3. The maximum travel distance as a function of rolling friction coefficient for spheres of different sizes moving on a horizontal plate with an initial velocity of 1 m/s, simulated by Method A (◯, 3 mm; △, 10 mm; ×, 30 mm) and Method B (□, 3 mm; ◇, 10 mm, +, 30 mm).

maximum distance becomes constant. This corresponds to the fact that for the cases considered, a large rolling friction coefficient will give a large rolling friction torque, which can stop any rotation almost instantaneously. In this case, this constant maximum distance is the same as that without any rotation.

### 3.2. Heap formation

Any practical processing of particulate materials involves a large number of particles. To examine the effectiveness of the proposed approach to such a multi-particle system, simulations of heap formation have been conducted under various conditions. It is known that if a heap is too small, the impact of oncoming particles may damage the

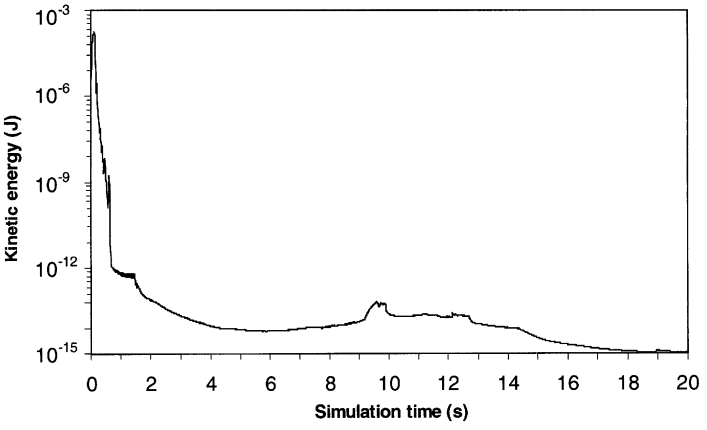


Fig. 4. Average kinetic energy per particle vs. simulation time for the settling of 10 mm spheres in a tube, when the rolling friction coefficients is $\mu_r = 10^{-4}$ m, simulated by Method A.

existing heap. To avoid this phenomenon, the present simulations are actually carried out under "cascading packing conditions" which have been successfully used in the previous laboratory scale experiments [38].

Thus, a simulation starts with the random generation of spheres of equal size in a small vertical cylindrical tube resting on a flat horizontal substrate, and there are no overlaps between the spheres, the tube wall and the flat substrate. The spheres are then allowed to settle under gravity for a period of time in the tube to form a packing. As shown in Fig. 4, it takes a long time for the spheres to completely lose their kinetic energy. On the other hand, trial tests indicate that as long as the settling time is not too short, it will not affect the heap formation much. Thus, the settling time used for the present work is 5 s. Then the tube was raised at a low speed, set to 0.015 m/s, allowing the spheres to spread and form an unconfined heap on the horizontal substrate. Since this work is focused on the effect of rolling friction coefficient, other physical properties are the same as those in Table 2. In this work, the particle–wall rolling friction coefficient is set to be double the particle–particle rolling friction coefficient, although the latter is referred to in all the following figures. The number of spheres in a simulation is constant, equal to 1000 for the results reported in this section, although simulations using much larger numbers, up to 10 000, have also been successfully carried out. Two-sized spheres are used, with their diameter equal to 10 or 3 mm, respectively. The diameter of the tube and the time step are 133 mm and $1.5 \times 10^{-5}$ s for large spheres, and 40 mm and $4 \times 10^{-6}$ s for small spheres.

Fig. 5 shows the variation of the average kinetic and potential energies of particles with time, obtained by means of Method A for large (10 mm) spheres. It can be observed that the energies both decrease with time after an initial stage in which the sharp decrease of potential energy results in an increase in the kinetic energy. The loss of the potential and kinetic energies is mainly due to the frictional and viscous

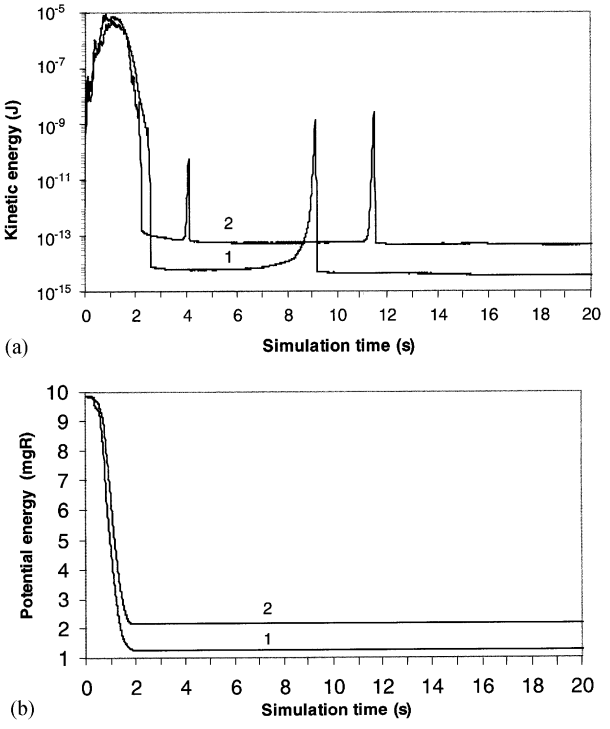


Fig. 5. Average kinetic (a) and potential (b) energies per particle as a function of simulation time for 10 mm spheres during formation of a heap for different rolling friction coefficients: line 1, $\mu_r = 5 \times 10^{-5}$ m; line 2, $\mu_r = 10^{-4}$ m, simulated by Method A.

damping effects in forming a heap. Physically, as the case for a single sphere moving on a plate discussed above, all spheres should loss their kinetic energy in order to form an absolutely stable heap. Numerically, this is difficult – if not impossible – to achieve. As seen in Fig. 5(a), after a very short period of time, a heap can reach a numerically stable stage, having a small but almost constant kinetic energy. This becomes obvious when examining the distribution of the kinetic energy that is constant after a short period (Fig. 6).

When examining the kinetic energy of individual particles, the situation would be more complicated. Each fluctuation observed in Fig. 5(a) corresponds to the occurrence of local instability resulting from the very slow movement and rearrangement of spheres. This high local instability is evident from Figs. 7 and 8(a) which show that the number of particles carrying 90% of the total kinetic energy at a fluctuation is extremely small, often just one or two particles. The reason for this is that the potential energy is much larger than the kinetic energy (Fig. 5); consequently, a small change in potential energy, e.g. a small decrease in the height of a single particle, may result in a large variation in kinetic energy. Without this local fluctuation, the kinetic energy is more uniformly distributed among the particles as shown in Fig. 8(b).

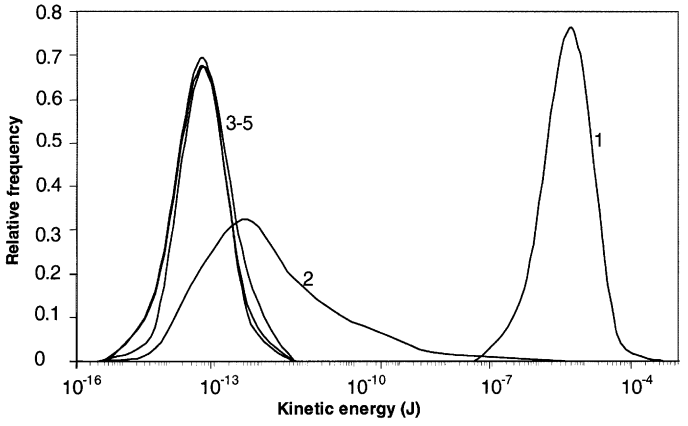


Fig. 6. Kinetic energy distribution in a heap of 10 mm spheres at different times: line 1, 1 s; line 2, 2 s; line 3–5 corresponding to 3 s, 10 s and 20 s; simulated by Method A with a rolling friction coefficient $\mu_r = 10^{-4}$ m.

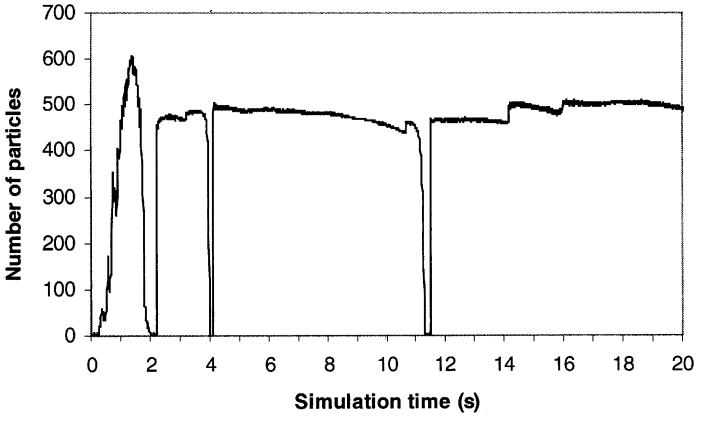


Fig. 7. Number of particles carrying 90% of the total kinetic energy as a function of simulation time for 10 mm spheres with a rolling friction coefficient of $\mu_r = 10^{-4}$ m, simulated by Method A.

As highlighted in Fig. 4, even under confined conditions, it is difficult to obtain an absolutely stable packing. The slow decay of kinetic energy, originated from the numerical nature of this type of dynamic simulation, is difficult to avoid. Therefore, the kinetic energy does not provide a reliable measure of the stability of a heap. On the other hand, it was found that in forming a heap, the potential energy of particles with respect to the horizontal substrate will decrease with time and finally reach a constant value. This feature is clearly observed in Fig. 5(b) where an essentially constant average potential energy is obtained within about 2 s for the cases considered. Consequently, the average potential energy is believed to be a better parameter to describe the stability of a heap. A high potential energy corresponds to a heap with a large angle of repose. If no heap is formed, the average potential energy will reach its minimum, equal to

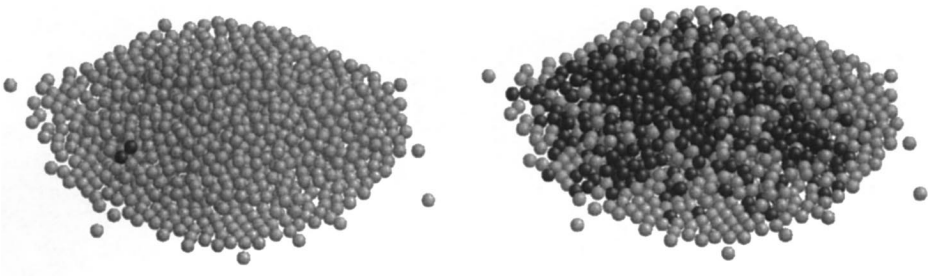

(a) (b)

Fig. 8. Number of particles (dark colour) carrying 90% of the total kinetic energy for 10 mm spheres: (a) with a fluctuation when $t = 11.6$ s; (b) without a fluctuation when $t = 12.0$ s; simulated by Method A when $\mu_r = 10^{-4}$ m.

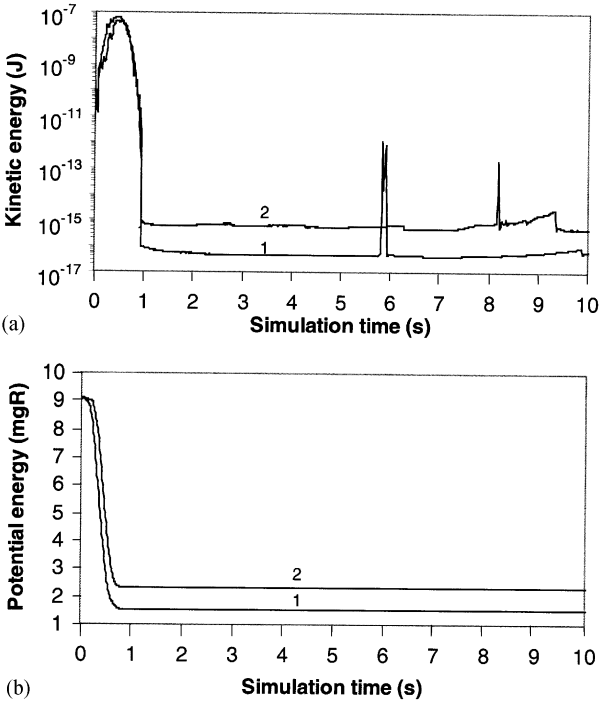


Fig. 9. Average kinetic (a) and potential (b) energies per particle as a function of simulation time for 3 mm spheres with different rolling friction coefficients in forming a heap: line 1, $\mu_r = 5 \times 10^{-5}$ m; line 2, $\mu_r = 10^{-4}$ m; simulated by Method A.

unity in units of mgR. Fig. 5 also suggests that a small rolling friction coefficient gives slightly small kinetic and potential energies for a stable heap. As shown in Fig. 9, this is also the case for small (3 mm) spheres.

The angles of repose is an important parameter in characterizing the heaping and internal friction behaviour of particulate materials. As shown in Figs. 10 and 11, it

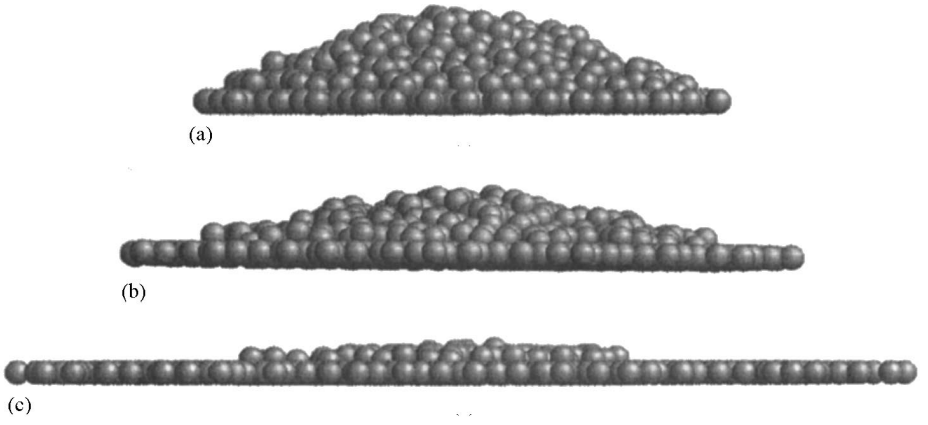


Fig. 10. Heaps of 10 mm spheres with different rolling friction coefficients: (a) $\mu_r = 2 \times 10^{-4}$ m; (b) $\mu_r = 10^{-4}$ m; (c) $\mu_r = 5 \times 10^{-5}$ m; simulated by Method A (simulation time =20 s).

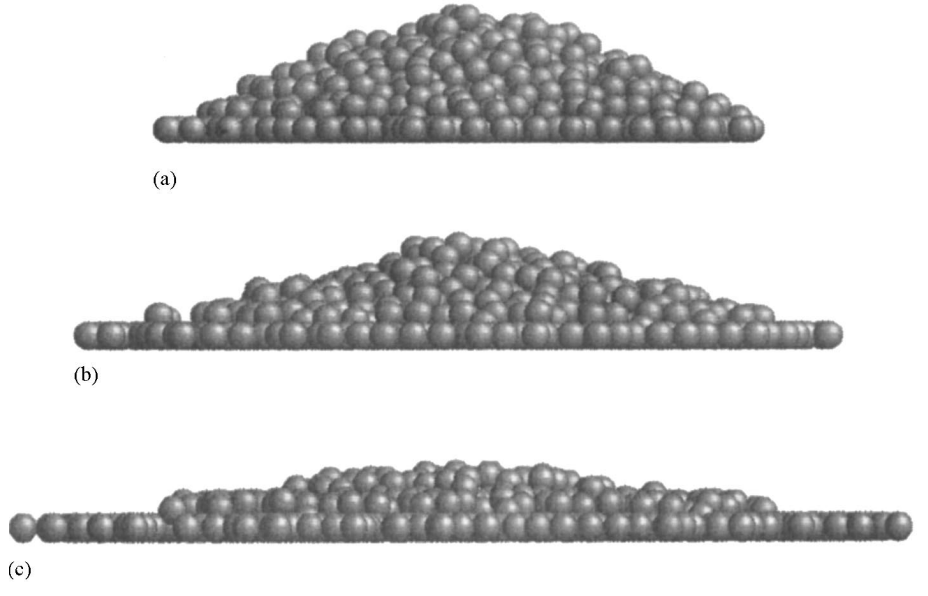


Fig. 11. Heaps of 3 mm spheres with different rolling friction coefficients: (a) $\mu_r = 10^{-4}$ m; (b) $\mu_r = 5 \times 10^{-5}$ m; (c) $\mu_r = 2.5 \times 10^{-5}$ m; simulated by Method A (simulation time =20 s).

strongly depends on the rolling friction coefficient, and a large rolling friction coefficient corresponds to a large angle of repose. Not surprisingly, no distinct heap can be formed if the rolling friction coefficient is too small, say, less than $10^{-5}$ under the present simulation conditions – a fact that explains why special constraints were necessary to form a stable heap in the previous studies [19–22]. Comparison of the results in Figs. 10 and 11 suggests that, consistent with experimental observation [39], the size

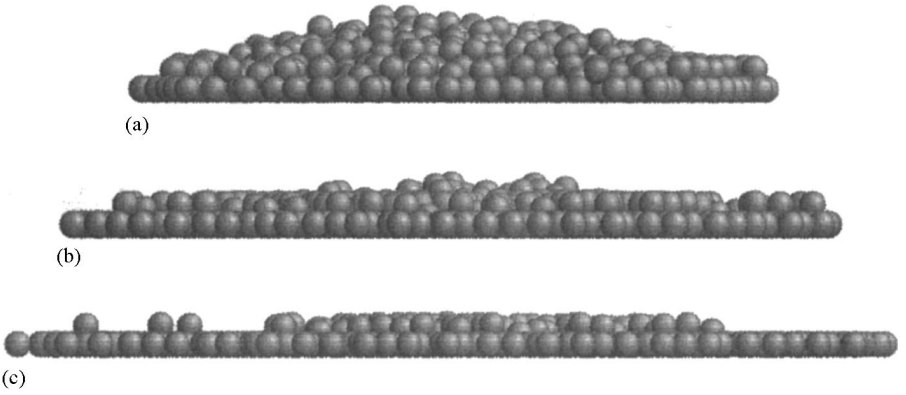


Fig. 12. Heaps of 10 mm spheres with different rolling friction coefficients: (a) $\mu_r' = 1$ s/rad; (b) $\mu_r' = 0.01$ s/rad; (c) $\mu_r' = 0.001$ s/rad; simulated by Method B (simulation time =20 s).

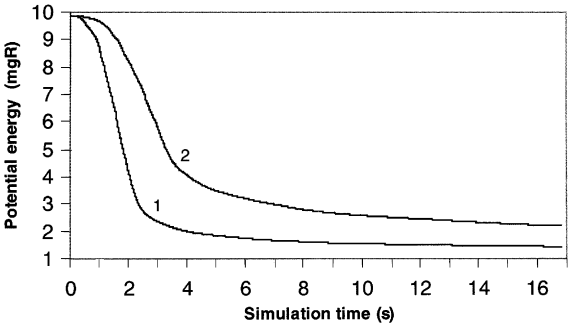


Fig. 13. Average potential energy per particle as a function of simulation time for 10 mm spheres forming a heap for different rolling friction coefficients: line 1, $\mu_r' = 0.01$ s/rad; line 2, $\mu_r' = 1$ s/rad; simulated by Method B.

of spheres also affects the angle of repose, with large spheres giving a small angle of repose. Similar trends can be observed if Method B is used (Fig. 12). However, it appears that this method is not as effective as method A, judged from the shape of a heap. In fact, as shown in Fig. 13, the average potential energy continues its decay even after a relatively long time of simulation.

A change of the angle of repose must correspond to a change of the internal stress distribution of a sandpile. The results in Figs. 10–12 indicate that under a given sandpiling condition, different rolling friction coefficients give different sandpile shapes and stress distributions. This will be studied in detail in future work.

### 3.3. Formation of a stagnant zone

A sandpile can also be formed inside a container after discharging particles, giving the so-called stagnant zone in unsteady hopper flow [40] or deadman in steady blast

furnace operation [41,42]. In fact, the present work stems from a failed attempt to simulate the existence of a deadman in a blast furnace by means of a dynamic simulation model without rolling friction [43]. Therefore, simulation of the formation of such a stagnant zone provides another test of the validity of the proposed approach, since the operational conditions are quite different.

For convenience, the present simulations are carried out with a rectangular container with two (side) outlets. Its geometrical details are shown in Fig. 14(a). The model parameters are the same as those used in the simulations described above (Table 2). A simulation is again started with the random generation of spheres in the container, followed with a gravitational settling process for 1.0 s to form a stable packing. Fig. 14(a) shows the results of such a packing, which is then used as the initial condition for discharging. The initial conditions include information about the positions and forces of all particles in the container, and for this particular simulation, the number of spheres used is 1154, with their diameter equal to 10 mm. Then, the instantaneous opening of the outlets starts a discharging process in which spheres flow into the bottom container under gravity, as illustrated in Figs. 14(b) and 14(c). Some spheres remain on the central plate after the discharging, forming a stable stagnant zone shown in Fig. 14(d).

As shown in Fig. 15, the kinetic energy averaged for the spheres above the central plate, after an initial instantaneous increase for transition from stationary to moving state, decreases gradually with time and then levels off after a sudden drop resulting from the discharging of the last batch of movable particles. Corresponding to the time for the drop, a stable stagnant zone is formed as indicated by the fact that the number of spheres on the central plate becomes almost constant, with a neglected decay (Fig. 16). Figs. 15 and 16 also suggest that large rolling friction coefficients can form stable stagnant zones faster. As expected, a larger rolling friction coefficient leads to more spheres in the stagnant zone and a larger angle of repose. Change of the sphere diameter will affect the results. As shown in Fig. 17, when the diameter is reduced from 10 to 6 mm, the number of remaining spheres increases from 186 to 974 when the rolling friction coefficient is $5 \times 10^{-6}$ m. The number of spheres used in the simulations differs (1154 for 10 mm spheres and 4000 for 6 mm spheres) in order that the initial height of the material in the container is nearly the same.

Fig. 18 shows the number of particles in the stagnant zone as a function of time, obtained by the use of Method B. Comparison with Fig. 16 confirms the idea that, from the point of view of simulation, Method B is not as effective as Method A in achieving a stable heap or stagnant zone. This is due to the fact that, according to Eq. (4), as the angular velocity decreases, the rolling friction torque also decreases, which leads to a long time for both to approach to zero and finally give a stable heap.

### *3.4. Comparison with experimental measurement*

To examine more quantitatively the validity of the proposed approach, experiments have been carried under conditions similar to those used in the simulation of the

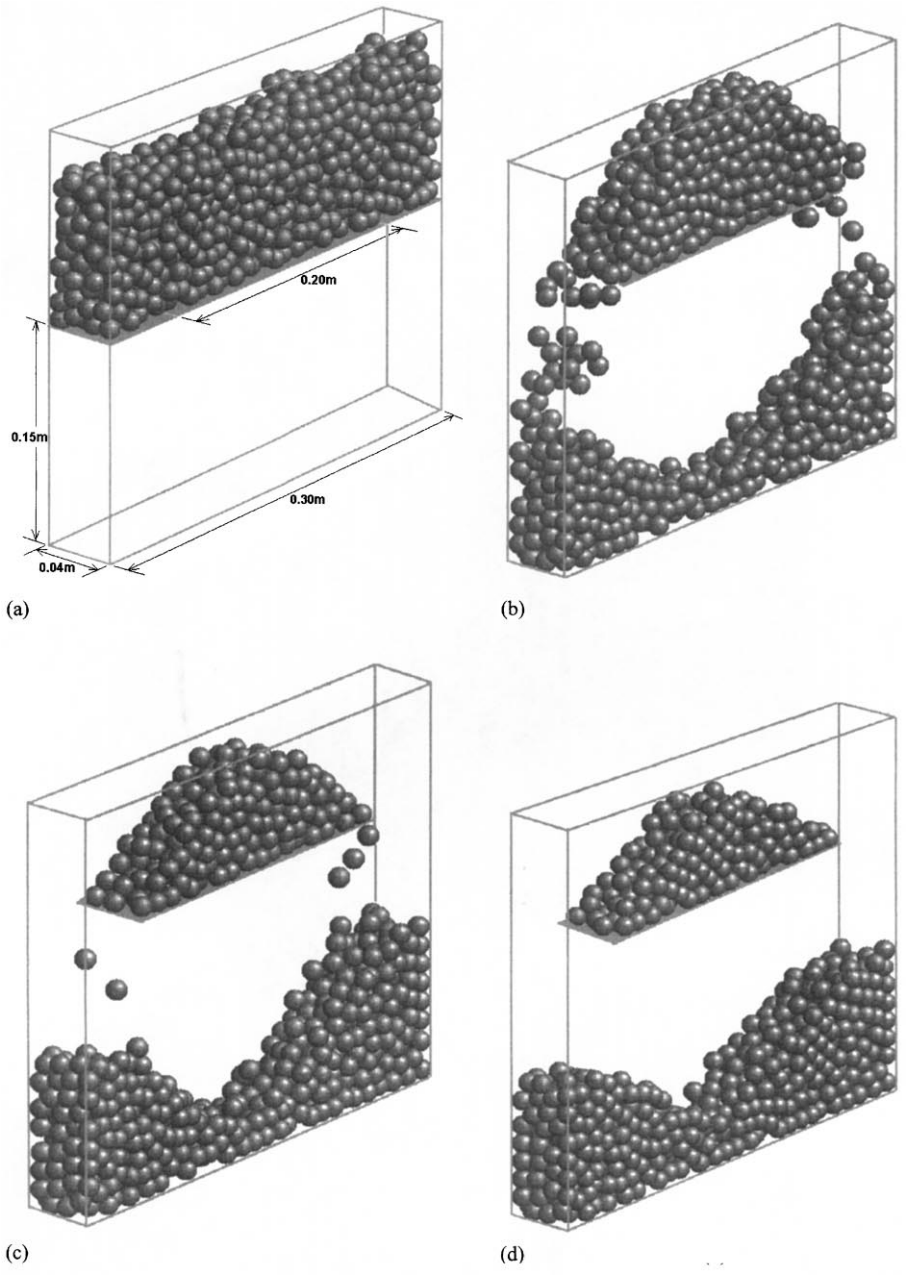


Fig. 14. Snapshots showing the formation of a stagnant zone for 10 mm spheres with a rolling friction coefficient of $\mu_r = 5 \times 10^{-5}$ m, at different discharge times: (a) $t = 0$ s; (b) 0.5 s; (c) 1.5 s; (d) 10.0 s, simulated by Method A.

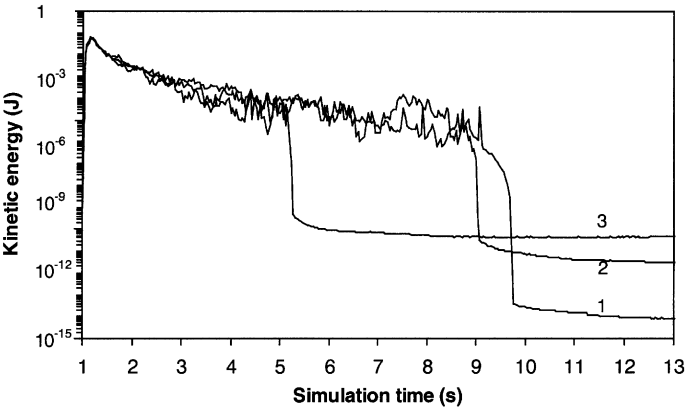


Fig. 15. Average kinetic energy per particle vs. simulation time for 10 mm spheres above the central plate obtained using different rolling friction coefficients: line 1, $\mu_r = 2.5 \times 10^{-5}$ m; line 2, $\mu_r = 5 \times 10^{-5}$ m; and line 3, $\mu_r = 10^{-4}$ m, simulated by Method A.

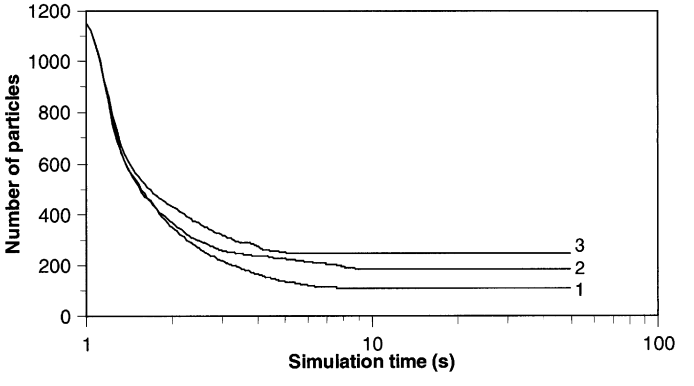


Fig. 16. Number of particles in a stagnant zone as a function of simulation time for 10 mm spheres with different rolling friction coefficients: line 1, $\mu_r = 2.5 \times 10^{-5}$ m; line 2, $\mu_r = 5 \times 10^{-5}$ m; and line 3, $\mu_r = 10^{-4}$ m, simulated by Method A.

formation of a stagnant zone. The geometry of the rectangular container is the same, although it is made of perspex, with a wooden block as the central plate. Glass beads with diameters of either 6 or 10 mm (particle density=2500 kg/m$^3$) are employed in the experiments. Figs. 19 and 20 show photographs of the stagnant zones, together with the simulated results, for the two sphere sizes, respectively. Obviously, the simulations are quite comparable with the measurements. In fact, the simulations with a rolling friction coefficient of $2.5 \times 10^{-5}$–$5 \times 10^{-5}$ m suggest that the number of spheres remaining on the centre plate is 125–186 for 10 mm spheres, and 752–974 for 6 mm spheres. These values are in good agreement with the experimental observations that the number of spheres in stagnant zone is $128 \pm 3$ for 10 mm spheres and $786 \pm 11$ for 6 mm spheres.

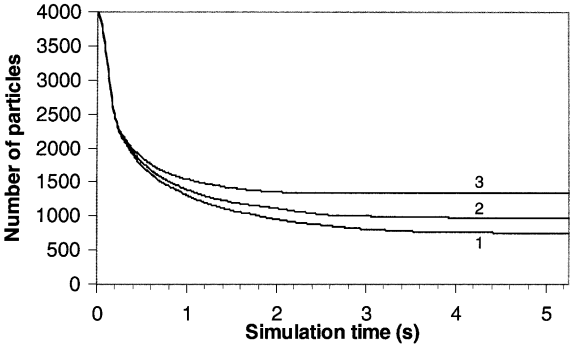


Fig. 17. Number of particles in a stagnant zone as a function of simulation time for 6 mm spheres with different rolling friction coefficients: line 1, $\mu_r = 2.5 \times 10^{-5}$ m; line 2, $\mu_r = 5 \times 10^{-5}$ m; and line 3, $\mu_r = 10^{-4}$ m, simulated by Method A.

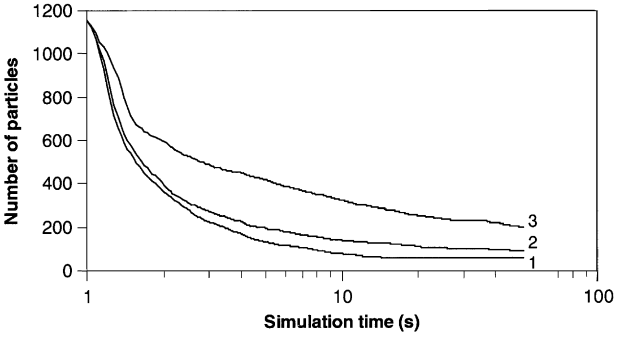


Fig. 18. Number of particles in a stagnant zone as a function of simulation time for 10 mm spheres with different rolling friction coefficients: line 1, $\mu_r' = 10^{-4}$ s/rad; line 2, $\mu_r' = 10^{-3}$ s/rad; and line 3, $\mu_r' = 10^{-1}$ s/rad, simulated by Method B.

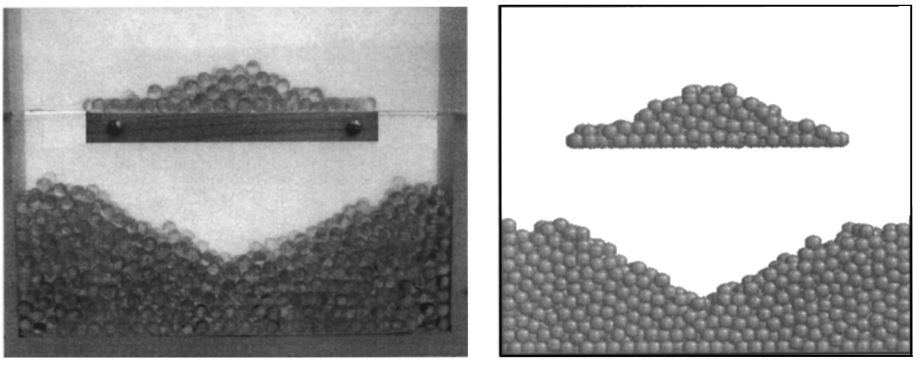

(a) (b)

Fig. 19. Stagnant zones formed by experiment and simulation for 1154 particles ($d$=10 mm); (a) experimental result; (b) simulation result by Method A ($\mu_r = 5 \times 10^{-5}$ m).

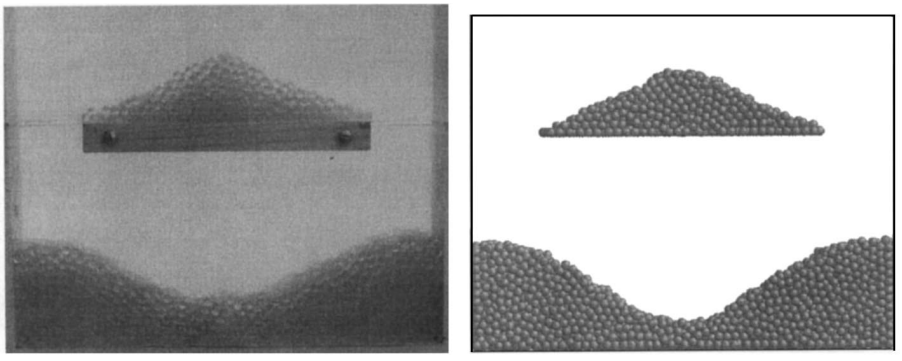

(a) (b)

Fig. 20. Stagnant zones formed by experiment and simulation for 4,000 particles ($d$=6 mm): (a) experimental result; (b) simulation result by Method A ($\mu_r = 5 \times 10^{-5}$ m).

## 4. Conclusions

Rolling friction, due to elastic hysteresis losses or viscous dissipation, has been incorporated in the dynamic simulation model developed by Cundall and Strack [17]. A numerical study of the formation of a heap of particles under different conditions indicates that the rolling friction plays a critical role in achieving physically or numerically stable results, and the angle of repose increases with rolling friction coefficient and decreases with particle size. While not clear from a theoretical point of view whether the rolling friction torque should be treated as angular velocity dependent or independent, the numerical results favour the latter. Comparison between the simulated and experimental results under comparable conditions confirms the validity of the proposed implementation. Successful simulation of the dynamic formation of sandpiles would provide an effective way to study their complex internal state.

## Acknowledgements

The authors would like to thank ARC and BHP for financial support, Dr. P. Zulli and Mr. S.J. Chew of BHP research and Prof. U. Tüzün of University of Surrey (UK) for helpful discussions, and Prof. P. Meakin of University of Oslo for helpful comments to enhance the quality of the paper.

## References

[1] L. Bates, User Guide to Segregation British Materials Handling Board press, United Kingdom, 1997, and many literatures therein.
[2] N. Standish, A.B. Yu, Q.L. He, Powder Technol. 68 (1991) 187.
[3] K. Liffman, D.Y.C. Chan, B.D. Hughes, Powder Technol. 78 (1994) 263.

[4] J. Grindlay, A.H. Opie, Phys. Rev. E 51 (1994) 718.
[5] P. Bak, C. Tang, K. Wiesenfeld, Phys. Rev. Lett. 59 (1987) 381.
[6] V. Frette, K. Christensen, A. Malthe-sorenssen, J. Feder, T. Jossang, P. Meakin, Nature 379 (1996) 49.
[7] H.A. Makse, S. Havlin, P.R. King, H.E. Stanley, Nature 386 (1997) 379.
[8] J. Baxter, U. Tüzün, D. Heyes, I. Hayati, P. Fredlund, Nature 391 (1998) 136.
[9] H.M. Jaeger, S.R. Nagel, Science 255 (1992) 1523.
[10] H.E. Stanley, E. Guyon (Series Eds.), Random Materials and Processes, Elsevier Science, Amsterdam.
[11] A. Mehta (Ed.), Granular Matters – An Interdisciplinary Approach, Springer, New York, 1994.
[12] R. Jullien, P. Meakin, Nature 344 (1990) 425.
[13] P. Meakin, R. Jullien, Physica A 180 (1992) 1.
[14] R. Jullien, P. Meakin, A. Pavlovitch, J. de Physique IV 3 (1993) 1981.
[15] E. Li, D.F. Bagster, Adv. Powder Technol. 3 (1992) 129.
[16] A. Mehta, Physica A 186 (1992) 121.
[17] P. Cundall, O.D.L. Strack, Geotechnique 29 (1979) 47.
[18] H.J. Herrmann, S. Luding, Continuum Mech. Thermodyn. 10 (1998) 189.
[19] J. Lee, H.J. Herrmann, J. Phys. A 26 (1993) 373.
[20] S. Luding, Phys. Rev. E 55 (1997) 4720.
[21] T. Elperin, E. Golshtein, Physica A 242 (1997) 332.
[22] J. Baxter, U. Tüzün, J. Burnell, D.M. Heyes, Phys. Rev. E 55 (1997) 3546.
[23] F.P. Beer, E.R. Johnson, Mechanics for Engineers – Statics and Dynamics, MacGraw-Hill, New York, 1976.
[24] N.V. Brilliantov, T. Poschel, Europhys. Lett. 42 (1998) 511.
[25] B.H. Xu, A.B. Yu, Chem. Eng. Sci. 52 (1997) 2786.
[26] K.L. Johnson, Contact Mechanics, Cambridge University press, Cambridge, 1985.
[27] O.R. Walton, Numerical simulation of inelastic, frictional particle-particle interactions, in: M.C. Roco (Ed.), Particulate Two-Phase Flow (Chapter 5), Butterworth-Heinemann, Boston, 1993.
[28] R.D. Mindlin, H. Deresiewicz, J. Appl. Mech. (Trans. ASME) 20 (1953) 327.
[29] C. Thornton, K.K. Yin, Powder Technol. 65 (1991) 153.
[30] D. Tabor, Philos. Mag. 43 (1952) 1055.
[31] D. Tabor, Proc. Roy. Soc. A 229 (1955) 198.
[32] J.A. Greenwood, H. Minshall, D. Tabor, Proc. R. Soc. London, Ser. A. 259 (1961) 480.
[33] J. Witters, D. Duymelinck, Am. J. Phys. 54 (1986) 80.
[34] I. Goryacheva, F. Sadeghi, Wear 184 (1995) 125.
[35] H. Sakaguchi, E. Ozaki, T. Igarashi, Int. J. Mod. Phys. B 7(9&10) (1993) 1949.
[36] K. Iwashita, M. Oda, J. Eng. Mech. 124 (1998) 285.
[37] P.A. Thompson, G.S. Grest, Phys. Rev. Lett. 67 (1991) 1751.
[38] A.B. Yu, D. Cowgill, P.L.M. Wong, N. Standish, Q.L. He, Stockpiling behaviour as observed in a model experiment, Proceedings of the 5th International Conference on Bulk Materials Storage, Handling and Transportation, Newcastle, Australia, 1995.
[39] J.T. Carstensen, P.C. Chan, Powder Technol. 15 (1976) 129.
[40] U. Tüzün, G.T. Houlsby, R.M. Nedderman, S.B. Savage, Chem. Eng. Sci. 37 (1982) 1691.
[41] S.J. Zhang, A.B. Yu, B. Wright, P. Zulli, U. Tüzün, ISIJ Int. 38 (1998) 1311.
[42] Y. Omori, Blast Furnace Phenomena and Modeling, Elsevier Applied Science, London, 1987.
[43] B.D. Wright, Formation of stagnant zones during discrete particle simulations of flowing solids, BHP Research & Technology Development Note; N98/021, 29 June 1998.